Aust. J. Phys., 1996, **49**, 527–41

Interaction of Highly Charged Ions with Surfaces*

Joachim Burgdörfer, Carlos Reinhold, Lotten Hägg and Fred Meyer

Physics Department, University of Tennessee,
Knoxville, TN 37996-1200, USA.
Oak Ridge National Laboratory, Oak Ridge, TN 37831-6377, USA.

Abstract

An overview is given of recent advances in the theoretical description of the interaction of multiply charged ions with surfaces. Simulations are presented displaying the formation of hollow atoms when slow highly charged ions approach the surface. It is shown that above-surface neutralisation proceeds via hollow-atom formation. Relaxation of the multiply excited states to the ground state occurs only subsequent to the close encounter with the topmost atomic layer.

1. Introduction

With the advent of high-current, highly charged ($Q \gg 1$), low energy ion sources, the interaction of slow multiply charged ions with surfaces has developed into one of the most active areas in the field of particle–solid interactions. On the most fundamental level, its interest is derived from the complex many-body response of metal electrons to the strong Coulomb perturbation characterised by a large Sommerfeld parameter $\eta = Q/v \gg 1$. The neutralisation is a true multi-electron capture (and loss) process involving up to the order of $\approx$100 electrons and posing a considerable challenge to theory. Furthermore, resonant transfer processes involve highly excited levels in the ion and are expected to set in at large distances from the surfaces when the Rydberg wavefunction begins to 'touch' the surface. The study of the multiply and highly charged ion–surface interaction is also of considerable importance for the understanding of surface damage and plasma–wall interactions.

We will briefly review the neutralisation scenario as originally proposed by Arifov *et al.* (1973) and discuss new experimental and theoretical results which have expanded our understanding of highly charged ion (HCI) surface interactions. The key element will be the classical 'over-barrier' model for electron transfer into Rydberg states (Burgdörfer *et al.* 1991; Burgdörfer 1993; Burgdörfer and Meyer 1993).

* Refereed paper based on a contribution to the Advanced Workshop on Atomic and Molecular Physics, held at the Australian National University, Canberra, in February 1995.

0004-9506/96/020527$05.00

2. The Ladder Model and the 'Bottleneck'

In 1973, Arifov and coworkers proposed an intriguing 'scenario' for the neutralisation of highly charged ions approaching a metallic surface and for the relaxation of large amounts of potential energy carried into the collision (Fig. 1). The first step is a multi-electron transfer into high n states by resonant 'tunneling' through the potential barrier. As soon as two or more electrons are localised in the projectile step-wise (intra)atomic Auger decay sets in. The Auger decay occurs most likely to a nearby n level with which the wavefunction still significantly overlaps and for which the energy gap is small. As a result, the Auger relaxation occurs along a 'ladder sequence' and is accompanied by the emission of low-energy electrons. As the ion approaches the surface, an increasing fraction of the initial potential energy will be dissipated by electron emission and, concurrently, the ion relaxes to its neutral ground state.

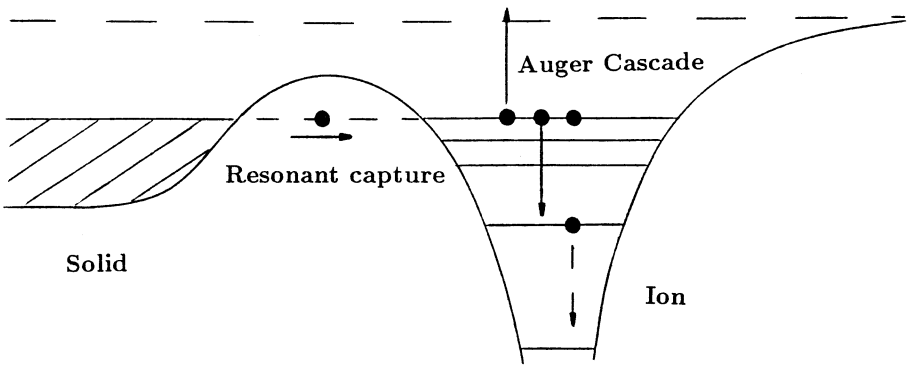

Fig. 1. Scenario for neutralisation and relaxation of multiply charged ions (Arifov *et al.* 1973).

While qualitatively very instructive, this 'ladder' model faces on a more quantitative basis a fundamental difficulty often referred to as the 'bottleneck' problem: Simple arguments illustrate that Auger rates for the decay of highly excited states are, by far, too slow to allow for the complete relaxation to the ground state along the ladder sequence. Consequently, the ion hits the surface long before the Auger relaxation is complete. The disparity of time scales for electron transfer to highly excited states and for Auger rates is at the core of the 'bottleneck problem'. One important consequence of the poor efficiency of the relaxation mechanism is the transient 'pile up' of electrons in a multiply excited state. Such an exotic configuration with an accumulation of electrons in high n shells, while the inner shells remain sparingly populated or empty, is called a 'hollow' atom. First direct evidence for hollow atom formation in ion–surface collisions was offered by the K X-ray satellite spectrum in argon (Briand *et al.* 1990) where individual satellite lines could be clearly identified as K_α transitions in the presence of a sparingly populated L shell but significant population in the M shell (and presumably higher shells). While the origin of this spectrum turned out to be primarily the subsurface formation of hollow atoms, it displays many features typical of hollow atoms formed above the surface.

3. Classical Over-barrier Model

The classical over-barrier (COB) model was originally developed for one-electron capture into highly charged ions in ion–atom collisions by Ryufuku *et al.* (1980) based on earlier work by Bohr and Lindhard (1954) and later extended by Barany *et al.* (1985) and Niehaus (1986) to incorporate multi-electron transfer. Its extension to ion–surface collisions (Burgdörfer *et al.* 1991; Burgdörfer and Meyer 1993) provides a simple framework for the description of ion–surface interactions. The physical significance of the COB model is derived from the fact that only classically allowed over-the-barrier processes as opposed to tunneling are sufficiently fast to be effective within the characteristic interaction time of the ion with the surface.

An 'active' electron at the position $\boldsymbol{r}$ crossing the barrier is subject to the potential

$$V(\boldsymbol{r}) = V_{pe}(|\boldsymbol{r} - R\hat{\boldsymbol{z}}|) + V_e(z) + V_{pe}^I(\boldsymbol{r}, R\hat{\boldsymbol{z}})\,, \tag{1}$$

where $\hat{\boldsymbol{z}}$ is the surface normal and $R\hat{\boldsymbol{z}}$ the position of the ion. Here V_{pe} is the direct interaction potential between the electron and the projectile,

$$V_{pe}(|\boldsymbol{r} - R\hat{\boldsymbol{z}}|) = \frac{-Q}{|\boldsymbol{r} - R\hat{\boldsymbol{z}}|}\,, \tag{2}$$

V_{pe}^I is the effective interaction of the electron with the projectile image,

$$V_{pe}^I = \frac{Q}{|\boldsymbol{r} + R\hat{\boldsymbol{z}}|}\frac{(\epsilon(\omega) - 1)}{(\epsilon(\omega) + 1)}\,, \tag{3}$$

and V_e is the effective interaction of the electron with the surface. Since the typical interaction time with the surface is $\simeq 10^{-14}$ s, the dynamic dielectric function $\epsilon(\omega)$ (Burgdörfer 1993) rather than the static dielectric constants (Barany and Setterlind 1995) should be used. For small distances, V_e should approach the bulk potential (i.e. the bottom of the conduction band), while for large distances it should approach an image-like limit

$$V_e \underset{z\to\infty}{=} \frac{-1}{4z}\frac{(\epsilon(\omega) - 1)}{(\epsilon(\omega) + 1)}\,. \tag{4}$$

Equations (3) and (4) are valid for insulators, semiconductors and metals. In the latter case, $|\epsilon(\omega)| \to \infty$ and the classical expressions for image potentials are recovered. The coordinate z_c of the barrier top is given by

$$V'(z_c) = 0 \tag{5}$$

and the barrier height by $V(z_c)$. A classical over-the-barrier transition takes place when the barrier top is lowered to the energy of the target levels,

$$V(z_c) = -W - \frac{2Q}{R(\epsilon(\omega) + 1)}\,, \tag{6}$$

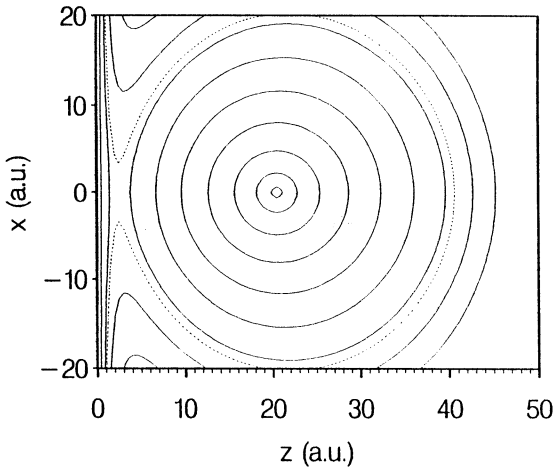

Fig. 2. Potential surface near saddle for an electron in the field of an N^{6+} ion at a distance $R = 20{\cdot}5$ a.u. from a gold surface. The dotted contour corresponds to the energy $\epsilon = -0{\cdot}17$ (from Burgdörfer *et al.* 1991).

where W is the workfunction of the target and the second term accounts for the shift of the target level in the field of the projectile. For metals and narrow band gap semiconductors $|\epsilon(\omega)|$ is large and the shift is negligible. When the condition (6) is satisfied, the equipotential contour corresponding to the workfunction extends now from the surface to the ionic core (Fig. 2). Since $V(z_c)$ is parametrically dependent on the distance R of the ion from the surface, (6) constitutes an implicit expression for the critical distance R_c where the first charge transfer takes place. Explicit expressions for R_c can be derived for asymptotic image potentials (3) and (4). For metals and narrow band gap semiconductors, one finds

$$R_c = \frac{\sqrt{2Q\epsilon(\omega)(\epsilon(\omega)-1)}}{W(\epsilon(\omega)+1)} + \frac{\epsilon(\omega)-1}{4W(\epsilon(\omega)+1)\epsilon(\omega)} + O(Q^{-1/2}). \tag{7}$$

For wide band gap insulators, the asymptotic image expression (4) for the electronic surface potential is inappropriate near the position of the saddle z_c which is typically of the order of 2 to 4 a.u. The direct Coulomb interaction of the electron with the residual vacancy in an ionic crystal is given by $-\alpha(z)/z$ where $\alpha(z)$ is related to an effective surface Madelung constant in the limit $z \to 0$, and the critical distance becomes

$$R_c = \frac{\sqrt{8\alpha(z_c)Q\epsilon(\omega)}}{W(\epsilon(\omega)+1)} + \frac{\alpha(z_c)}{W\epsilon(\omega)} + O(Q^{-1/2}). \tag{8}$$

Critical distances for the first charge transfer for a typical metal (gold) and a typical insulator (LiF) differ significantly from each other (Fig. 3). The COB model, furthermore, predicts the quantum number of the projectile level n_c which is populated by resonant charge transfer and is given by

$$n_c = Q_{\text{eff}} \Big/ \left[2\left(W + \frac{2Q}{R_c(\epsilon(\omega)+1)} + \frac{(Q-\frac{1}{2})}{2R_c}\frac{(\epsilon(\omega)+1)}{(\epsilon(\omega)-1)} - \frac{\alpha(R_c)}{R_c}\right)\right]^{\frac{1}{2}}. \quad (9)$$

For highly charged ions ($Q \gg 1$), $n_c \gg 1$, i.e. the capture proceeds into high Rydberg states whose energy is shifted due to the interaction with the surface at large distances

$$E_n = -\frac{Q_{\text{eff}}^2}{2n^2} + \frac{Q-\frac{1}{2}}{2R}\frac{\epsilon(\omega)-1}{\epsilon(\omega)+1} - \frac{\alpha(R)}{R}. \quad (10)$$

The term $-\alpha(R)/R$ describes the interaction between the projectile levels and the surface. As electrons are transferred from an insulator the surface is charged up and α increases. The effective charge Q_{eff} is defined in terms of Slater screening parameters taking into account the electrons previously transferred.

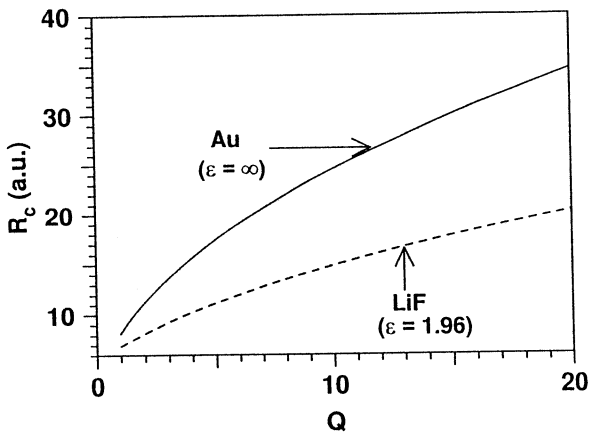

Fig. 3. Critical distance $R_c(Q)$ for first charge transfer as a function of the projectile charge Q. Solid curve, gold surface; dashed curve, lithium fluoride (LiF).

4. Simulation of the Neutralisation and Relaxation Cascade above the Surface

After the onset of the over-barrier flow of electrons from the conduction or valence band into the ionic potential well, the further evolution of the charge cloud is determined by the competition of three pathways: the capture of additional electrons into the ionic core which is now partially screened, the over-barrier resonant ionisation (the inverse process to capture) and Auger relaxation, i.e. intra atomic electron–electron scattering resulting in the relaxation of one electron and emission of a second electron.

The evolution of the excited states population can be simulated using a system of coupled rate equations which incorporates the physical picture outlined above. It describes the rate of change of the population of each n shell, $P_n(R)$, as a function of the instantaneous distance R. No distinction between different subshells is made since strong ℓ-mixing occurs near the surface in presence of the image field. The rate equations for $P_n(R)$ read (Burgdörfer *et al.* 1991)

$$v_z(R)\frac{d}{dR}P_n(R) = I_n^C(R) - I_n^L(R)P_n(R) + \tfrac{1}{2}\sum_{n'>n} A_{n,n'}P_{n'}^2(R) - P_n^2(R)\sum_{n'<n} A_{n',n}\,. \tag{11}$$

This set is augmented by the equation for the number of autoionised electrons $P_I(R)$,

$$v_z(R)\frac{d}{dR}P_I(R) = \tfrac{1}{2}\sum_{n'>n} A_{n,n'}P_{n'}^2(R)\,. \tag{12}$$

The evolution of the perpendicular velocity of the approaching ion is described by Newton's equation of motion for the image acceleration

$$\frac{d}{dR}v_z(R) = \frac{1}{\mu v_z(R)}\frac{\partial}{\partial R}V_p^I(R) \tag{13}$$

(μ is the mass of the ion). The image acceleration provides a lower limit on the perpendicular velocity v_z irrespective of the incident velocity $v_z^0 = \lim_{R\to\infty} v_z(R)$. The current of captured electrons, $I_n^C(R)$, plays the role of an inhomogeneous source term. The rate for resonant ionisation into the unoccupied band structure is denoted by $I_n^L(R)$. Both rates can be estimated from the corresponding geometric cross sections for over-barrier transitions and depend parametrically on the instantaneous charge state $Q(R)$ of the ion. The Auger rates can be estimated from rates for intrashell states (Burgdörfer *et al.* 1991; Cowan 1981):

$$A_{n,n'} = \frac{5{\cdot}06\times 10^{-13}}{\Delta n^{3\cdot 46}}\,. \tag{14}$$

This estimate applies to the subset of the fastest Auger decay rates in the highly excited ion. Only that subset is of significance since slowly decaying processes are suppressed by the competing reionisation channel.

5. Hollow Atoms above the Surface

Simulations employing rate equations (11)–(13) reproduce, indeed, the scenario of hollow atom formation above the surface. Fig. 4 illustrates the formation of hollow atoms for Ar^{12+} on a gold surface (Lemell 1994). We emphasise the dynamical, transient nature of this process. With decreasing distance from the surface, the n levels shift upward in energy due to the image interaction (10) and screening by electrons already transferred to the ion. Highly excited states continuously decay by resonant ionisation and intra-atomic Auger processes. This results in a continuous shift of the population to lower n shells. Fig. 5 illustrates schematically the evolution of the position and population of levels as the ion approaches the surface.

Recent experiments offer complementary evidence for the transient formation of hollow atoms. Winter *et al.* (1993) and Aumayr *et al.* (1993) measured the image acceleration for a wide range of charge states up to $Q = 79$ and provided

direct evidence for the charge state evolution of the ion and for the characteristic distances (6) where the electron transfer takes place. In other words: the experiment measures to what extent the ion is neutralised, as seen from the surface. Recent K Auger data (Meyer *et al.* 1991; Das *et al.* 1992; Köhrbrück *et al.* 1994) and X-ray data (Andrä *et al.* 1992; D'Etat *et al.* 1992), on the other hand, measure the amount and rate of filling of the L shell, or equivalently, how empty inner shells of the incident ions are, prior to hitting the surface.

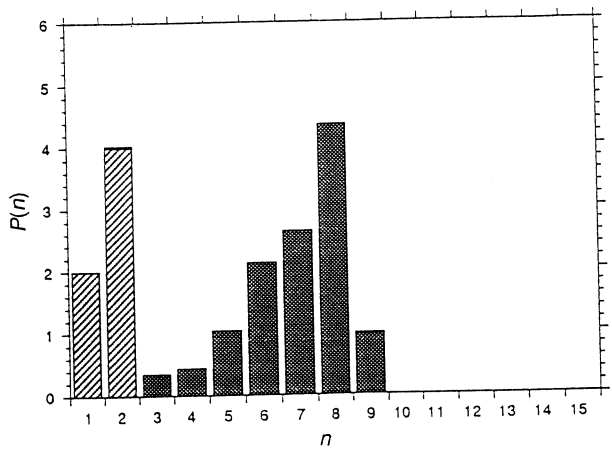

Fig. 4. Population distribution over n shells in Ar^{12+} impacting on a gold surface with a nominal energy of 21 eV (the actual impact energy is increased by image acceleration). The atom is fully neutralised but hollow.

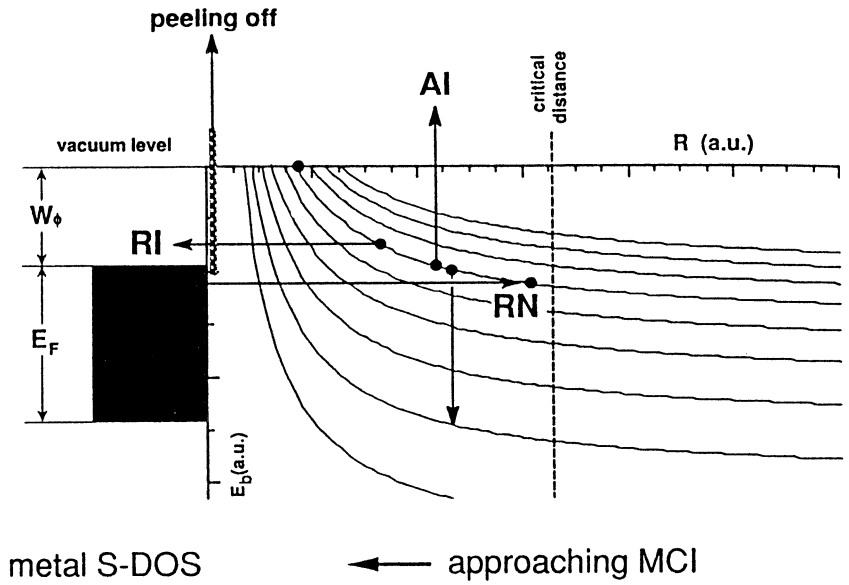

Fig. 5. Charge transfer into energy shifted projectile levels as the highly charged ion approaches a surface (schematically). RN: resonant neutralisation; RI: resonant ionisation; and AI: autoionisation.

The essence of the physical picture underlying the energy gain by image acceleration can be captured in terms of a simple analytic estimate based on a simplified version of the COB model which turns out to be remarkably accurate (Burgdörfer and Meyer 1993). Assuming instantaneous charge transfer and complete screening of the projectile charge by the captured electron, the effective charge will be reduced to $Q-1$ at the distance $R_c(Q)$ and will be constant until the critical distance $R_c(Q-1)$ is reached, where the charge state is reduced to $Q-2$ etc. Fig. 6 displays the staircase-like charge state evolution for Ar^{6+} approaching an Al surface, underlying this estimate. The resulting energy gain due to the interaction of the ion with its own image for a metal surface, $-Q^2/4R$, summed over all steps of the staircase, is given by

$$\Delta E = \frac{W}{4}\sum_{i=0}^{Q-1}\frac{2(Q-i)-1}{\sqrt{2(Q-i)}}. \tag{15}$$

In the limit of large Q, the sum in (15) can be converted to an integral, yielding the asymptotic expansion in Q

$$\Delta E = \frac{W}{2\sqrt{2}}[\tfrac{2}{3}Q^{\frac{3}{2}} - \tfrac{3}{4}Q^{\frac{1}{2}} + 0{\cdot}521] + O(Q^{-1/2}). \tag{16}$$

Equation (16) approximates (15) to within 3% for charge states as low as $Q=6$. The numerical simulation according to (11)–(13) agrees with the staircase quite well even though differences are noticeable. The resulting image acceleration reproduces the experimental data over a wide range of charge states up to $Q=79$ (Fig. 7) (Aumayr *et al.* 1993).

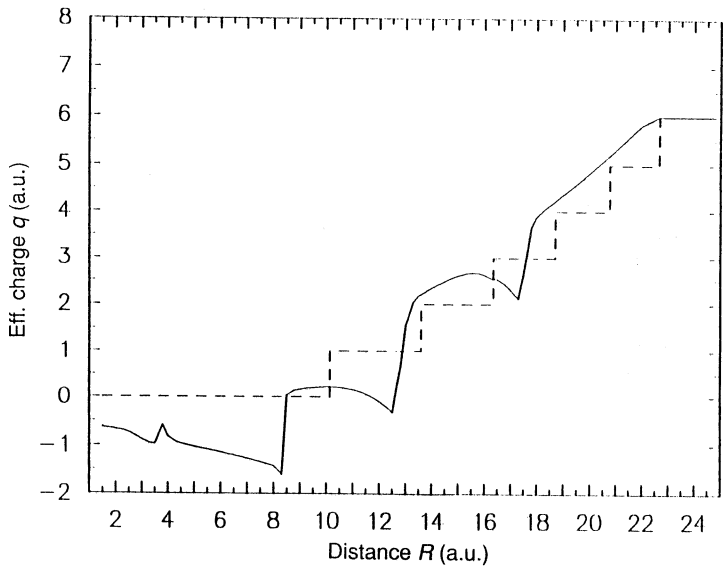

Fig. 6. Effective charge state Q_{eff} as a function of the distance from the surface. Solid curve: simulation using the classical-over-barrier model, dashed line: staircase model (see text).

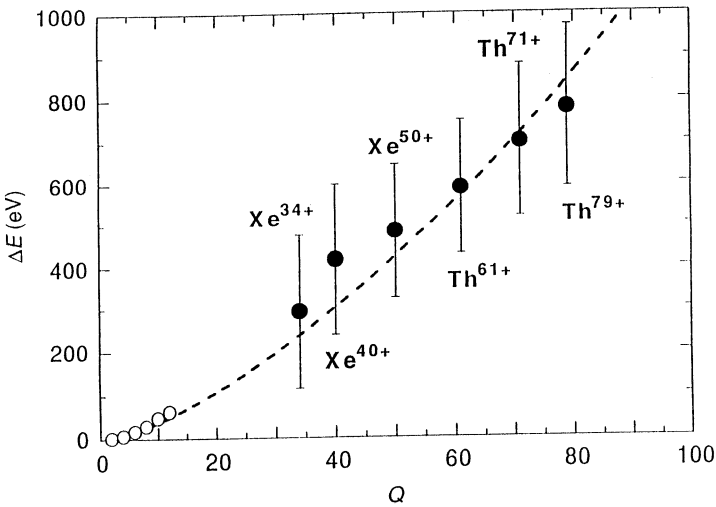

Fig. 7. Image acceleration as a function of the charge of the impinging ion from Aumayr *et al.* (1993), where the dashed curve is the $Q^{\frac{3}{2}}$ scaling (equation 16).

6. Neutralisation and Relaxation at the Surface

Contrary to the implications of the original ladder cascade model, the projectile hits the surface in a state far away from its neutral electronic ground state. A significant fraction of the potential energy carried into the collision remains to be dissipated. The outer charge cloud of the hollow atom gets 'peeled off' upon impact, part of which will be emitted as secondary electrons while the dominant fraction will be transferred to unoccupied states of the solid. Estimates on the fraction of peeled off electrons backscattered from the surface range from 20 to 50% (Lemell *et al.* 1995).

The filling of inner and moderately excited shells of the projectile occurs in close binary collisions with surface and below surface atoms. It is at this stage where the second generation of 'hollow atoms', observed in the X-ray spectrum by Briand *et al.* (1990), is being formed. It is worth while noting that very similar X-ray spectra from hollow atoms inside the solid have been observed much earlier (Kauffman *et al.* 1976; Raman and Vane 1984) produced, however, by a different process: multiple ionisation of target atoms by highly charged energetic projectiles followed by rapid charge transfer from the valence band and neighbouring atoms creates very slow 'hollow' target recoil atoms which relax by X-ray emission and Auger decay. Dependencies on the valence electron density and electronegativity of target atoms were found ('chemical effects'), which can be understood as resulting from quasi-resonant charge transfer into a hollow atom very similar to the neutralisation of multiply charged ions at the surface.

The quantitative simulation of the relaxation of second-generation hollow atoms at surfaces is still in its infancy. Very recently, experimental data for the neutralisation of surface-channeled multiply charged ions have become available (Folkerts *et al.* 1995). For collisions at small angles of grazing incidence θ, surface penetration can be ruled out. Moreover, with the help of trajectory simulations

for surface channeling which reproduce the angular distribution of the scattered particles, a well-defined window for the interaction time with the surface could be established (in the present case $\sim 3\times 10^{-14}$ s). For this relatively simple case, a simulation of the experimentally observed neutralisation, relaxation and even negative ion formation near the topmost layer could be performed (Burgdörfer *et al.* 1995). The basic physical ingredient for the fast filling of the inner shells is the matching of length and energy scales between target and projectile electronic states due to screening by the medium. Resonant matching also provides a simple explanation of the 'universality' of fast neutralisation which has been observed for several projectiles, charge states, and target surfaces (Winter *et al.* 1993; Folkerts *et al.* 1995), that is, its independence of the energy levels of the projectile or specific target properties. The scale matching can be appropriately summarised by the statement 'everything is about one atomic unit'. Specifically, the screening radius of an electron gas of metallic density is given in the Thomas–Fermi approximation by (Kittel 1971)

$$a_{\mathrm{TF}} = 0{\cdot}641\, r_s^{\frac{1}{2}}\,, \tag{17}$$

where r_s is the Wigner–Seitz radius ($2 \leq r_s \leq 6$ for metals), and a_{TF} is of the order of 1 a.u. Furthermore, since a_{TF} is only very weakly dependent on the electron density ($\propto n^{-1/6}$), it essentially reaches the bulk value at the topmost layer of the surface. For multiply charged ions ($Q \gg 1$) and lower lying shells ($n \approx 2$) the atomic shell radius

$$\langle r\rangle_n = n^2/Q \tag{18}$$

is small compared to 1 a.u. in vacuum. However, due to the screening by the electron gas, the effective charge seen by the electron bound to the projectile near the surface becomes a function of the distance r between the electron and the projectile with the limits

$$\lim_{r\ll a_{\mathrm{TF}}} Q(r) = Q_0 \gg 1, \qquad \lim_{r\gg a_{\mathrm{TF}}} Q(r) = 0\,, \tag{19}$$

where Q_0 is the effective charge state in the absence of screening. Consequently, there exists an upper limit of n for which the electron remains bound which corresponds to the outermost shell of the second generation of 'hollow atoms'. This cut-off is determined by the matching of the orbital radius and the screening length

$$a_{\mathrm{TF}} \simeq \langle r\rangle_{n,q} \approx 1\,. \tag{20}$$

This qualitative picture can be made more quantitative by a simple approximation to the energy shift near the surface using the linearised Thomas–Fermi approximation for an inhomogeneous electron gas, by allowing the electron density $n(R)$ and, hence, $r_s(R)$ to be a function of the distance R from the surface, measured from the topmost layer. This treatment of the inhomogeneous density near the surface is similar to the uniform density approximation (UDA) (Stott and Zaremba 1980; Norskov and Lang 1980). An electron bound at a distance r from projectile

which is located at a distance R from the surface experiences a partially screened Coulomb field. The bare charge is reduced by the induced charge $q_{\rm ind}$ which is given in the linear Thomas–Fermi approximation by

$$q_{\rm ind}(R,r) = q_0[1 - e^{-r/a_{\rm TF}(R)}(1 + r/a_{\rm TF}(R))]\,, \tag{21}$$

where isotropic screening is assumed in line with the UDA model. At the shell radius, $r = \langle r\rangle$, (21) will determine the Slater-type 'inner' screening charge for the electronic orbit. Combining (18) with (21) leads to a simple self-consistency relation for the hydrogenic orbitals

$$\frac{n^2}{q_0 a_{\rm TF}(R)} = (x + x^2)e^{-x}\,, \tag{22}$$

where $x = \langle r\rangle_n / a_{\rm TF}(R)$. This self-consistent relation determines not only for a given n, q_0 and R the effective shell radius and the orbital energy, but also gives a stability limit beyond which the projectile can no longer hold on to the electron. Equation (22) can be easily extended to the multi-electron systems of hollow atoms. For equivalent electrons an additional term describing the partial expulsion of screening charge (self-screening or 'Fermi hole') must be included on the right-hand side. Non-equivalent 'inner' electrons can be included by reducing the core charge q_0 by the number of inner, non-equivalent electrons N_i.

The shift of the energy value calculated with this simplified TF method interpolates smoothly between the asymptotic vacuum value and the bulk value. Despite its inherent oversimplification, it permits the determination of energy shifts at the surface with an adequate level of accuracy as compared to density-functional calculations (Arnau 1994; Arnau *et al.* 1995). Fig. 8 displays the binding energy of the outermost electron for the configurations $(K^1L^k, k = 1,\ldots 8)$ with one core hole in O^{q+} in front of a gold surface. No distinction is made between different ℓ states. The strong upward shift of even the lowest lying $O^{6+}(K^1L^1)$ state brings this level into resonance with the $5s$ and $5p$ levels of gold whose positions in the Hartree–Fock approximation are also displayed. The COB model also takes into account the energy shift of localised target states due to the projectile, not shown in Fig. 8.

Using the position dependent energy levels as input, a classical simulation for quasi-resonant charge transfer at the surface employing the classical over-the-barrier model has been performed. The present treatment is an extension of the theory for above-surface neutralisation (Section 3). Since the COB model indicates that the above atomic surface neutralisation is very inefficient to fill the L shell ($\langle n_L\rangle < 1$), the L shell is treated as being empty near the point of closest approach and only the direct sequential charge transfer into configurations $(K^1L^k, k = 1,\ldots 8)$ with the K shell hole present and into ground state configurations $(K^2L^k, k = 1,\ldots 7)$ including the negative ion state is included. The occupation numbers of the rate equations refer now to configurations rather than shells. The corresponding level diagram for the projectile M shell (not shown) indicates that in the initial stage of the near-surface interaction direct quasi-resonant filling of the M shell is also possible. However, this route is not the dominant pathway because of the slow additional Auger decay required for subsequent filling of the L shell. Since the COB model employs the classical continuum approximation to low-lying levels

separated by relatively wide level spacings, quasi-resonant processes include also the subset of two-centre Auger transitions for which the energy transfer to the second electron is smaller than the bin size ΔE associated with each quantum level.

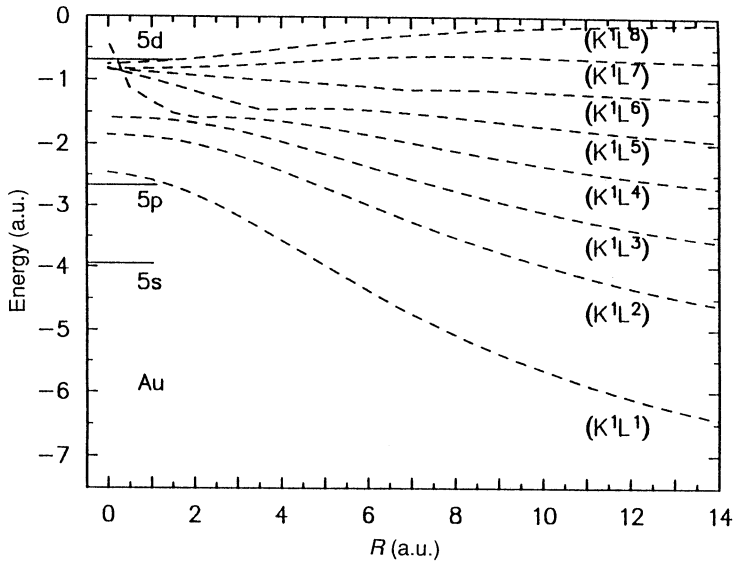

Fig. 8. Orbital energies of outermost electrons of the configurations (K^1L^k) in oxygen with one hole in the K shell as a function of the distance from the surface (topmost atomic layer).

Fig. 9*a* shows the evolution of a selected number of charge states O^{q+} as a function of the coordinate x parallel to the surface ($x = 0$ is the point of closest approach). Fig. 9*b* displays a 'typical' trajectory for grazing incidence scattering (Niehof and Heiland 1990; Folkerts *et al.* 1995), with points of closest approach $1 \lesssim R_0 \lesssim 1{\cdot}5$ a.u. The initial state $O^{7+}(1s)$ becomes almost instantaneously depleted as soon as the resonance condition for over-the-barrier transitions is satisfied. The population is rapidly transferred to core excited levels $O^{q+}(KL^k)$, an example of which ($k = 4$) is also shown in Fig. 9. The ground state configurations $O^{q+}(K^2L^k)$ become filled within the characteristic time for Auger decay, shown here for $k = 4$–7. The negative ion state, $k = 7$, dominates in the vicinity of the surface which is converted into the neutral atom ($k = 6$) by resonant ionisation on the outgoing path. The simulation yields for $R \to \infty$ almost complete neutralisation (typically 80 to 95%). These results are in excellent agreement with the experimental data by Folkerts *et al.* (1995), also shown in Fig. 9. Fractions of negative ion formation of similar magnitude have been observed also in other laboratories (Kessel *et al.* 1994; Hughes *et al.* 1994; Briere *et al.* 1994). It is worth while pointing out that the almost complete neutralisation and relaxation is largely independent of the choice of the parameters entering the classical over-the-barrier model. This remarkable result is due to the fact that the time interval within which the ion is in close contact with the surface (dwell time 3×10^{-14} s within 2Å or 4 a.u. from the topmost layer) is of the order of the Auger decay time. The latter is, however, much

larger (at least one order of magnitude) than the characteristic time for charge transfer. This dissimilarity of time scales yields the weak dependence on the detailed values of the capture and loss rates which, in turn, lends credence to the results of the oversimplified COB model.

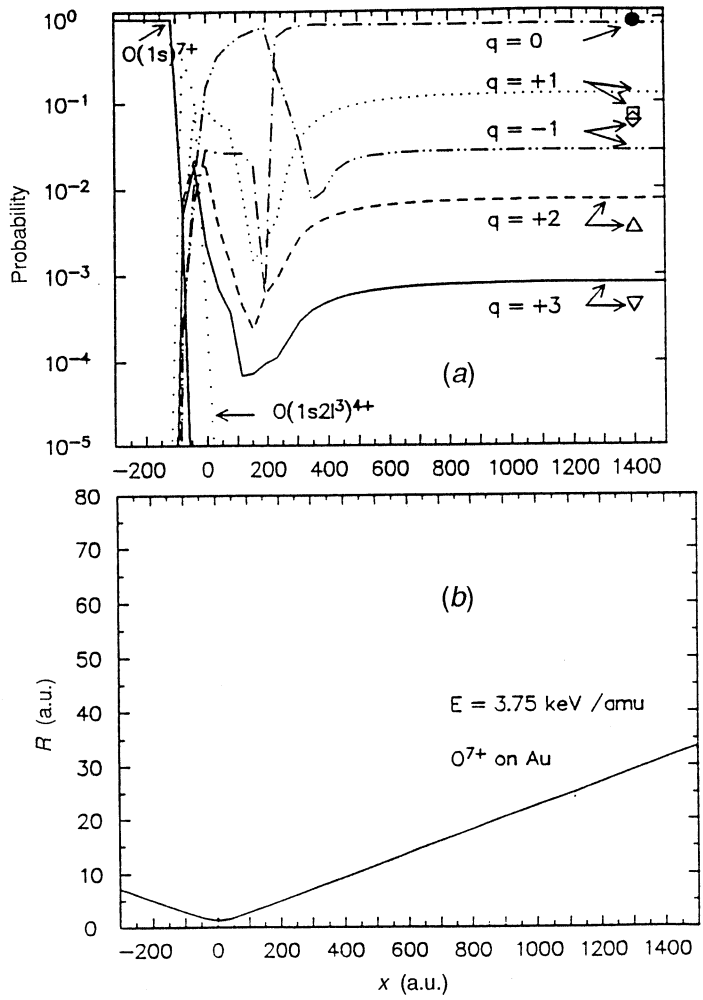

Fig. 9. Evolution of the charge state during grazing incidence scattering of $O^{7+}(1s)$ at the gold surface: (a) $(\theta = 1{\cdot}8°, E = 3{\cdot}75$ keV/amu) as a function of the coordinates parallel to the surface (in a.u.), where $x = 0$ at the point of closest approach; (b) the trajectory for specular reflection.

7. Summary

Considerable progress has been achieved in our understanding of highly charged ion–surface interactions. The presently accepted scenario for metals supported by several experiments involves three stages (Burgdörfer *et al.* 1991; Aumayr and Winter 1994). During the first stage (I), the highly charged ion approaching the

surface is accelerated by its own image charge and, at a critical distance R_c, begins to extract electrons from the metal surface. These electrons are captured resonantly into highly excited states of the projectile, eventually forming a neutral but 'hollow atom', which subsequently decays via autoionisation and other above surface electron emission mechanisms. Because the image charge attraction limits the available interaction time, even at the lowest initial projectile energies, the autoionisation cascade cannot be completed outside the solid. Screening of the projectile core by metal electrons near the surface (phase II) results in the 'peeling off' of the still weakly bound projectile electrons. Decay of inner shell vacancies of the projectile near the topmost layer at or inside the solid (phase III) leads to the emission of X rays or fast Auger electrons which can also produce slow secondary electrons by cascade effects. The dissipation of the ~keV potential energy is complete only after the ion undergoes close collisions with surface and subsurface atoms. Many open questions remain: They include the origin of differences between metals and insulators, the role of two-electron processes and of electron correlation. Development of a quantum treatment of this multi-electron process remains a challenge to theory.

Acknowledgment

This work was supported in part by the National Science Foundation and by the US Department of Energy, Office of Basic Energy Sciences, Division of Chemical Sciences, under Contract No. DE-AC05–840R21400 with Martin Marietta Energy Systems, Inc.

References

Andrä, H. J., Simionovici, A., Lamy, T., Brenac, A., Lamboley, G., Pesnelle, A., Andriamonje, S., Fleury, A., Bonnefoy, M., Chassevent, M., and Bonnet, J. J. (1992). ICPEAC XVII, Brisbane, Australia (1991), Invited Papers, p. 98.

Arifov, U. A., Mukhamadiev, E. S., Parilis, E. S., and Pasuyk, A. S., (1973). *Zh. Tekh. Fiz.* **43**, 375 [Arifov, U. A., Kishinesvskii, L. M., Mukhamadiev, E. S., and Parilis, E. S., *Sov. J. Tech. Phys.* **18**, 203 (1973)].

Arnau, A. (1994). Personal communication.

Arnau, A., Zeijlmans van Emmichoven, P. A., Juaristi, J. I., and Zaremba, E. (1995). *Nucl. Instr. Meth.* B **100**, 279.

Aumayr, F., Kurz, H., Schneider, D., Briere, M. A., McDonald, J. W., Cunningham, C. E., and Winter, H. P. (1993). *Phys. Rev. Lett.* **71**, 1943.

Aumayr, F., and Winter, H. P. (1994). *Comments At. Mol. Phys.* **29**, 275.

Barany, A., Astner, G., Cederquist, H., Danared, H., Huldt, S., Hvelplund, P., Knudsen, H., Liljeby, L., and Rensfelt, K. (1985). *Nucl. Instr. & Meth.* B **9**, 397.

Barany, A., and Setterlind, C. (1995). *Nucl. Instr. & Meth.* B **98**, 184.

Bohr, N., and Lindhard, J. (1954). *Dan. Vid. Sel. Mat. Phys. Medd.* **78**, No. 7.

Briand, J. P., *et al.* (1990). *Phys. Rev. Lett.* **65**, 159.

Briere, M. A., *et al.* (1994). *Nucl. Instr. & Meth.* B **90**, 231.

Burgdörfer, J. (1993). 'Review of Fundamental Processes and Applications of Atoms and Ions' (Ed. C. D. Lin), pp. 517–614. (World Scientific: Singapore).

Burgdörfer, J., Lerner, P., and Meyer, F. W. (1991). *Phys. Rev.* A **44**, 5674.

Burgdörfer, J., and Meyer, F. W. (1993). *Phys. Rev.* A **47**, R20.

Burgdörfer, J., Reinhold, C., and Meyer, F. (1995). *Nucl. Instr. & Meth.* B **98** 415.

Cowan, R. D. (1981). 'Theory of Atomic Structure and Spectra' (University of California Press: Berkeley).

Das, J., Folkerts, L., and Morgenstern, R. (1992). *Phys. Rev.* A **45**, 4669.

D'Etat, B., Briand, J. P., Ban, G., de Billy, L., Briand, P., Desclaux, J. P., Melin, G., Lamy, T., Lamboley, G., Richard, P., Stockli, L. M., Ali, R., Renard, N., Schneider, D., Clark, M., Beiersdorfer, P., and Decaux, V. (1992). HCI Invited Papers, Manhattan, Kansas.
Folkerts, L., Schippers, S., Zehner, D. M., and Meyer, F. W. (1995). *Phys. Rev. Lett.* **74**, 2204.
Hughes, I., *et al.* (1994). Seventh Int. Conf. on the Physics of Highly Charged Ions, Vienna, Austria.
Kauffman, R., Jamison, K., Gray, T., and Richard, P. (1976). *Phys. Rev. Lett.* **36**, 1074.
Kessel, Q., *et al.* (1994). Seventh Int. Conf. on the Physics of Highly Charged Ions, Vienna, Austria.
Kittel, C. (1971). 'Introduction to Solid State Physics' (Wiley: New York).
Köhrbrück, R., Grether, M., Spieler, A., Stolterfoht, N., Page, R., Saal, A., and Bleck-Neuhaus, J. (1994). *Phys. Rev.* A **50**, 1429.
Lemell, C. (1994). Diploma Thesis, TU Wien.
Lemell, C., Winter, H. P., Aumayr, F., Burgdörfer, J., and Reinhold, C. (1995). *Nucl. Instr. & Meth.* B **102**, 33.
Meyer, F. W., Overbury, S. H., Havener, C. C., Zeijlmans van Emmichoven, P. A., Burgdörfer, J., and Zehner, D. M. (1991). *Phys. Rev.* A **44**, 7214.
Niehaus, A. (1986). *J. Phys.* B **19**, 2925.
Niehof, A., and Heiland, W. (1990). *Nucl. Inst. & Meth.* B **48**, 306.
Norskov, J. K., and Lang, N. D. (1980). *Phys. Rev.* B **21**, 2131.
Raman, S., and Vane, C. (1984). *Nucl. Instr. & Meth.* B **3**, 71 and references therein.
Ryufuku, H., Sasaki, K., and Watanabe, T. (1980). *Phys. Rev.* A **21**, 7451.
Stott, M., and Zaremba, E. (1980). *Phys. Rev.* B **22**, 1564.
Winter, H., Auth, C., Schuch, R., and Beebe, E. (1993). *Phys. Rev. Lett.* **71**, 1939.

Manuscript received 15 February, accepted 21 June 1995